Instability due to cross-phase modulation in the normal-dispersion regime

M. Yu and C. J. McKinstrie

Department of Mechanical Engineering, University of Rochester, Rochester, New York 14627
and Laboratory for Laser Energetics, 250 East River Road, Rochester, New York 14623

Govind P. Agrawal

The Institute of Optics, University of Rochester, Rochester, New York 14627

The interaction of two light waves, having different frequencies and propagating in a dispersive non-linear medium, is studied using the method of Zakharov (Zh. Eksp. Teor. Fiz. **51**, 1107 (1966) [Sov. Phys. JETP **24**, 740 (1967)]). This method does not require the sidebands of the incident waves to have frequencies comparable to those of the incident waves, as do the coupled nonlinear Schrödinger equations that are normally used to model this interaction. It is shown that cross-phase modulation does not necessarily lead to instability of the incident waves. In particular, two light waves propagating in the normal-dispersion regime of a conventional single-mode fiber are stable. However, cross-phase-induced modulational instability can occur in a conventional fiber when one of the light waves propagates in the anomalous dispersion regime. The dispersion curve associated with a dispersion-flattened fiber has two regions in which dispersion is normal, separated by a region in which dispersion is anomalous. Cross-phase-induced modulational instability can occur in a dispersion-flattened fiber when the two light waves propagate in different normal-dispersion regimes.

PACS number(s): 42.81.Dp, 52.35.Mw, 42.65.Ky

I. INTRODUCTION

The propagation of two intense light waves that have different frequencies, in a single-mode optical fiber, is usually studied within the framework of coupled nonlinear Schrödinger (NS) equations. These equations have been used to predict several interesting phenomena [1], including the cross-phase-induced modulational instability in the normal-dispersion regime [2–4]. Although such an instability has been observed when cross-phase modulation occurs between the two polarization components of a single wave [5], no such instability has ever been observed by using two pump waves that have the same polarization, but different frequencies. Two assumptions made in the derivation of the coupled NS equations are that the waves have narrow spectra centered on their respective carrier frequencies and that the coherent four-wave-mixing (FWM) interaction between two incident waves can be neglected [6,7]. The self-consistency of the predicted phenomena and these assumptions must always be checked.

An alternative approach to nonlinear wave interactions has been developed by Zakharov [8]. This approach does not require the wave spectra to be narrow or the non-linear coupling coefficients to be independent of frequency. It has been applied to the study of several instabilities in fluids [8–10] and plasmas [8,11], and is well suited to the study of the aforementioned optical interaction. Such an analysis shows that cross-phase modulation is not a sufficient condition for the existence of instability in the normal-dispersion regime. Specifically, the importance of the effects of cross-phase modulation on the incident waves depends on the form of the dispersion curve and

the incident-wave frequencies.

The outline of this paper is as follows. The Zakharov equation, upon which all subsequent analysis is based, is introduced in Sec. II. In Sec. III an equilibrium solution of the Zakharov equation is found and linear equations governing the evolution of small perturbations of this equilibrium are derived. The consequences of these equations are investigated in Sec. IV, for light waves in both conventional and dispersion-flattened fibers, and for several different combinations of pump frequencies. Finally, in Sec. V, the main results of the paper are summarized.

II. ZAKHAROV EQUATION

Consider wave propagation in a single-mode fiber. The electric field is written as

$$\overline{E}(t,\mathbf{r}) = \overline{A}(t,z)\overline{F}(x,y) ,\qquad (2.1)$$

where $\overline{A}$ is referred to as the wave amplitude and the function $\overline{F}$ describes the transverse variation of the field. The Fourier amplitude of the wave is defined according to the convention

$$A(\omega,z) = \frac{1}{2\pi} \int_{-\infty}^{\infty} \overline{A}(t,z)\exp(i\omega t)dt .\qquad (2.2)$$

With this notation, the mode-coupling, or Zakharov, equation [8] takes the form

$$[d_z - i\beta(\omega)] A(\omega,z) = i \int_{-\infty}^{\infty} \int_{-\infty}^{\infty} \int_{-\infty}^{\infty} \gamma(\omega;\omega',\omega'',\omega''') A(\omega',z) A(\omega'',z) A(\omega''',z) \delta(\omega-\omega'-\omega''-\omega''') d\omega' d\omega'' d\omega''' ,$$

$$(2.3)$$

where $\beta(\omega)$ is the linear wave number corresponding to the frequency ω. To within a factor of order unity that depends on the transverse mode structure, the nonlinear coupling coefficient is given, in electrostatic units, by

$$\gamma(\omega;\omega',\omega'',\omega''') = \frac{2\pi\omega\chi^{(3)}(\omega;\omega',\omega'',\omega''')}{cn(\omega)A_{\text{eff}}} , \qquad (2.4)$$

where $\chi^{(3)}(\omega;\omega',\omega'',\omega''')$ is the third-order nonlinear susceptibility of the fiber, $n(\omega)$ is its refractive index, and A_{eff} is its core area [1]. In the limit of narrow bandwidth, the Zakharov equation (2.3) reduces to the NS equation. Both equations require nonlinearity to be weak and to produce spatial variation of the Fourier amplitudes on a scale long compared to an optical wavelength. All stimulated processes, such as Brillouin and Raman scattering, are excluded.

III. HARMONIC ANALYSIS

Suppose that the input field is given by

$$A(\omega,0) = \sqrt{P_1}[\delta(\omega-\omega_1)+\delta(\omega+\omega_1)]$$
$$+ \sqrt{P_2}[\delta(\omega-\omega_2)+\delta(\omega+\omega_2)] , \qquad (3.1)$$

corresponding to two pump waves of peak "power" $2P_1$ and $2P_2$. Without loss of generality, $\omega_1 < \omega_2$. The evolution of A with distance is determined by the Zakharov equation (2.3). Because the input Fourier spectrum is discrete, the integrations in the Zakharov equation reduce to summations. A simple analysis of this equation shows that the nonlinear terms on the right-hand side are of two types: incoherent self- and cross-plane modulation terms, which produce nonlinear wave-number shifts at the input frequencies, and coherent coupling terms, which transfer energy to other frequencies, such as $3\omega_2$, $2\omega_2+\omega_1$, and $2\omega_2-\omega_1$.

Since the generated waves all require a considerable distance to grow to finite amplitude, the initial evolution of the input field can be determined by retaining in the Zakharov equation only those Fourier components associated with the two pump frequencies. At the frequency ω_1, the Zakharov equation reduces to

$$[d_z - i\beta(\omega_1)] A(\omega_1,z) = i\gamma(P_1+2P_2) A(\omega_1,z) , \qquad (3.2)$$

where a degeneracy factor of 3 has been included in definition (2.4) and $\gamma(\omega_1;\omega_1,\omega_2,-\omega_2)$ has been assumed comparable to $\gamma(\omega_1;\omega_1,\omega_1,-\omega_1)$. Throughout this paper, γ will be assumed to depend only weakly on frequency and its arguments will be omitted for simplicity of notation. Should the need arise, it is not difficult to extend the analysis of this paper to include the frequency dependence of γ. The solution of Eq. (3.2) is

$$A(\omega_1,z) = \sqrt{P_1} \exp[i\phi_1(z)] ,$$
$$\phi_1(z) = \beta(\omega_1)z + \gamma(P_1+2P_2)z . \qquad (3.3)$$

A similar analysis shows that

$$A(\omega_2,z) = \sqrt{P_2} \exp[i\phi_2(z)] ,$$
$$\phi_2(z) = \beta(\omega_2)z + \gamma(2P_1+P_2)z . \qquad (3.4)$$

Solutions (3.3) and (3.4) represent two pump waves with nonlinear wave-number shifts and are valid near the entrance to the fiber. When the amount of energy transferred to the generated waves is small, they are also globally valid equilibrium solutions of the Zakharov equation. Due to the frequency dependence of the refractive index, this condition is usually satisfied for third-harmonic and sum-frequency generation. However, the generation of light at the difference frequency $2\omega_2-\omega_1$, which is close to ω_2 if the incident frequencies are not too dissimilar, warrants further investigation. From the Zakharov equation,

$$[d_z - i\beta(2\omega_2-\omega_1)] A(2\omega_2-\omega_1,z)$$
$$= i\gamma P_2\sqrt{P_1} \exp[i2\phi_2(z)-i\phi_1(z)]$$
$$+ i2\gamma(P_1+P_2) A(2\omega_2-\omega_1,z) . \qquad (3.5)$$

In the undepleted pump-wave approximation, the solution of Eq. (3.5) is facilitated by writing

$$A(2\omega_2-\omega_1,z) = B(z) \exp[i\beta(2\omega_2-\omega_1)z$$
$$+ i2\gamma(P_1+P_2)z] . \qquad (3.6)$$

It follows immediately that

$$B(z) = (\gamma P_2\sqrt{P_1}/\delta\beta)[\exp(i\delta\beta z)-1] , \qquad (3.7)$$

where

$$\delta\beta = 2\beta(\omega_2)-\beta(\omega_1)-\beta(2\omega_2-\omega_1)-\gamma(2P_2-P_1) \qquad (3.8)$$

is the total (linear plus nonlinear) wave-number mismatch of this particular generation process. Thus, the energy transfer due to pump-pump FWM will be minimal provided that

$$\left| \frac{2\gamma P_2}{2\beta(\omega_2)-\beta(\omega_1)-\beta(2\omega_2-\omega_1)-\gamma(2P_2-P_1)} \right| \ll 1 .$$

$$(3.9)$$

Inequality (3.9) requires the wave-number mismatch (3.8) to be much larger than the nonlinear coupling term in Eq. (3.5) to suppress difference-frequency generation. When this condition is satisfied, the nonlinear term can be omitted from the denominator of inequality (3.9). A similar inequality follows from the consideration of light generation at the difference frequency $2\omega_1-\omega_2$.

Suppose that inequality (3.9) is satisfied and, hence, that Eqs. (3.3) and (3.4) describe an equilibrium solution of the Zakharov equation. To study the stability of this equilibrium, one should linearize the Maxwell and polar-

ization equations underlying the Zakharov equation around the equilibrium solution. To the order of accuracy of the Zakharov equation, this procedure is equivalent to linearizing the Zakharov equation itself. However, one can avoid a formal linearization of the Zakharov equation by using harmonic analysis: Due to the intrinsic linearity of the stability analysis, any perturbation of the equilibrium can be decomposed into small-amplitude waves at various frequencies. Consequently, one only needs to study the evolution of each group of small-amplitude waves. These waves are referred to as "sidebands" of the pump waves because the frequencies of any unstable group are close to the pump frequencies, as will be demonstrated.

Consider the evolution of a probe wave of frequency $\omega_1+\omega$. Suppose first that $\omega \gg \omega_2-\omega_1$. In this case, the interaction of the probe and pump waves produces harmonics whose amplitudes are much smaller than the probe amplitude. Although the probe wave is subject to a nonlinear wave-number shift, its energy is essentially undepleted. This harmonic generation is similar to that described above, except that the probe wave contributes one of the driving components on the right-hand side of the Zakharov equation.

Conversely, suppose that $\omega \sim \omega_2-\omega_1$. In this case, some of the generated waves can be nearly phase matched. One example is the wave generated at the frequency $\omega_1+\omega_2-(\omega_1+\omega)=\omega_2-\omega \sim \omega_1$. For these waves, the wave-number-mismatch terms are comparable to, or smaller than, the nonlinear coupling terms. Hence, they can be driven to amplitudes as large as the probe amplitude. In turn, these generated waves modify the probe wave. Consequently, the evolution of the entire group of waves must be determined self-consistently. Notice that this scenario automatically includes the previous scenario as a special case.

The second scenario is now considered in detail. Suppose that the probe wave has frequency $\omega_1+\omega$, where $|\omega| < (\omega_2-\omega_1)/2$. Only those sidebands at the frequencies $\omega_1-\omega$, $\omega_2+\omega$, and $\omega_2-\omega$ can be driven near resonantly, unless special arrangements are made to allow other FWM processes to occur. This situation is illustrated in Fig. 1. When $(\omega_2-\omega_1)/2 < |\omega| < 3(\omega_2-\omega_1)/2$, the interaction is identical to the preceding interaction. To see
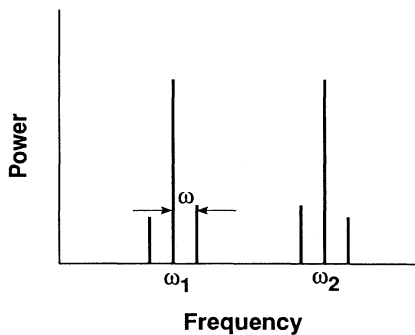

FIG. 1. Fourier spectrum of the electric field. The large peaks represent the two pump waves, whereas the four small peaks represent the four sidebands whose evolution is coupled by the nonlinearities in the Zakharov equation (2.3).

this, suppose that $\omega > (\omega_2-\omega_1)/2$ and define $\omega'=(\omega_2-\omega_1)-\omega$. Then $\omega_1+\omega=\omega_2-\omega'$, with $|\omega'| < (\omega_2-\omega_1)/2$, and the probe wave should be regarded as a sideband of the higher-frequency pump wave (unless, of course, the pump waves are orthogonally polarized). However, the physics of the interaction is unaltered, as stated. When $|\omega| > 3(\omega_2-\omega_1)/2$, the other sidebands are usually driven nonresonantly and, hence, the interaction is usually stable. Consequently, in the following analysis, the frequency difference between the probe and the lower-frequency pump wave is assumed to satisfy the inequality

$$|\omega| < (\omega_2-\omega_1)/2 \ . \tag{3.10}$$

Furthermore, the symmetry of the sideband frequencies allows one to restrict the four-sideband analysis to positive values of ω.

The derivation of the sideband evolution equations from the Zakharov equation is straightforward. Just as the pump waves are subject to nonlinear wave-number shifts, so also are the sidebands. In anticipation of these wave-number shifts, it is convenient to define

$$A(\omega_1+\omega,z)=B_{1+} \exp[ikz+i\phi_1(z)] \ ,$$
$$A(\omega_1-\omega,z)=B_{1-} \exp[-ik^*z+i\phi_1(z)] \ ,$$
$$A(\omega_1+\omega,z)=B_{2+} \exp[ikz+i\phi_2(z)] \ , \tag{3.11}$$
$$A(\omega_2-\omega,z)=B_{2-} \exp[-ik^*z+i\phi_2(z)] \ .$$

The sideband equations then take the form

$$D_{1+}(\omega,k)B_{1+}=\gamma P_1(B_{1+}+B_{1-}^*)$$
$$+2\gamma\sqrt{P_1P_2}(B_{2+}+B_{2-}^*) \ ,$$
$$D_{1-}(\omega,k)B_{1-}^*=-\gamma P_1(B_{1+}+B_{1-}^*)$$
$$-2\gamma\sqrt{P_1P_2}(B_{2+}+B_{2-}^*) \ ,$$
$$D_{2+}(\omega,k)B_{2+}=\gamma P_1(B_{2+}+B_{2-}^*) \tag{3.12}$$
$$+2\gamma\sqrt{P_1P_2}(B_{1+}+B_{1-}^*) \ ,$$
$$D_{2-}(\omega,k)B_{2-}^*=-\gamma P_1(B_{2+}+B_{2-}^*)$$
$$-2\gamma\sqrt{P_1P_2}(B_{1+}+B_{1-}^*) \ ,$$

where the dispersion functions

$$D_{1+}(\omega,k)=k-\beta(\omega_1+\omega)+\beta(\omega_1) \ ,$$
$$D_{1-}(\omega,k)=k+\beta(\omega_1-\omega)-\beta(\omega_1) \ ,$$
$$D_{2+}(\omega,k)=k-\beta(\omega_2+\omega)+\beta(\omega_2) \ , \tag{3.13}$$
$$D_{2-}(\omega,k)=k+\beta(\omega_2-\omega)-\beta(\omega_2) \ .$$

The physical significance of these equations can be seen as follows: Suppose that the nonlinear terms in Eqs. (3.3) and (3.12) are absent. Then, from the second of Eqs. (3.3) and the first of Eqs. (3.11)–(3.13),

$$A(\omega_1+\omega,z)=B_{1+} \exp[i\beta(\omega_1)z+ikz] \ , \tag{3.14}$$

where

$$k=\beta(\omega_1+\omega)-\beta(\omega_1) \tag{3.15}$$

and the probe wave propagates with its natural wave number. Thus, the term $\beta(\omega_1+\omega)-\beta(\omega_1)$ is the linear mismatch between the natural wave number of the probe wave and the wave number at which it is driven by the terms on the right-hand side of the mode-coupling equation, when they are present. The four-sideband interaction described by Eqs. (3.12) and (3.13) can be unstable. The spatial growth rate of this instability depends on the nonlinear coupling between the sidebands, which tends to be destabilizing, and the intrinsic linear and nonlinear wave-number shifts of each sideband, which tend to be stabilizing.

By combining Eqs. (3.12), one can show that

$$[D_{1+}D_{1-}+\gamma P_1(D_{1+}-D_{1-})]$$

$$\times[D_{2+}D_{2-}+\gamma P_2(D_{2+}-D_{2-})]$$

$$=4\gamma^2 P_1 P_2(D_{1+}-D_{1-})(D_{2+}-D_{2-}) . \quad (3.16)$$

The solutions of this instability dispersion equation depend on the shape of the fiber dispersion curve and, in general, must be determined numerically. The relative amplitudes of the sidebands then follow from Eqs. (3.12) and (3.13). For the limit in which $\omega \ll \omega_2-\omega_1$, Eq. (3.16) reduces to the usual dispersion equation that is derived from coupled NS equations [2–4].

IV. RESULTS AND DISCUSSION

Three different cases are illustrated in Fig. 2. Consider first Figs. 2(a) and 2(b), for which both pump frequencies are in the normal or anomalous dispersion regime of a conventional single-mode fiber and are not too close to the zero dispersion point. Suppose that the dispersion curve can be approximated by a parabola over the frequency range $[\omega_1-(\omega_2-\omega_1)/2,\omega_2+(\omega_2-\omega_1)/2]$. Such a parabola can be characterized by its first derivative $d\beta/d\omega=\beta_1$ and second derivative $d^2\beta/d\omega^2=\beta_2$ evalu-
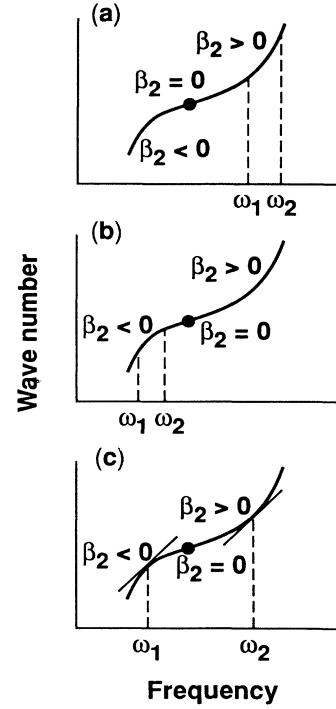

FIG. 2. Dispersion curve of a conventional fiber. (a) Both pump frequencies are in the normal-dispersion regime. (b) Both pump frequencies are in the anomalous-dispersion regime. (c) One pump frequency is in the normal-dispersion regime and the other pump frequency is in the anomalous-dispersion regime. Notice that the pump frequencies can be chosen in such a way that the pump-wave group velocities are equal.

ated at ω_1. Although this parabolic approximation cannot be made for all dispersion curves, it serves to illustrate the physics of the interaction. For equal pump powers, the dispersion equation (3.16) becomes

$$\{[k-\beta_1\omega]^2-(\beta_2\omega^2/2)[2\gamma P+(\beta_2\omega^2/2)]\}\{[k-\beta_1\omega-(\omega_2-\omega_1)\beta_2\omega]^2-(\beta_2\omega^2/2)[2\gamma P+(\beta_2\omega^2/2)]\}$$

$$=(4\gamma P)^2(\beta_2\omega^2/2)^2 , \quad (4.1)$$

while condition (3.9) for the absence of pump-pump FWM becomes

$$\left|\frac{2\gamma P}{(\omega_2-\omega_1)^2\beta_2}\right|\ll 1 . \quad (4.2)$$

Analysis of Eq. (4.1) is facilitated by the change of variables

$$K=\frac{k-\beta_1\omega}{\gamma P} , \quad C=\mathrm{sgn}(\beta_2) ,$$

$$S=\left|\frac{(\omega_2-\omega_1)^2\beta_2}{2\gamma P}\right|^{1/2} , \quad \Omega=\left|\frac{\beta_2\omega^2}{2\gamma P}\right|^{1/2} >0 . \quad (4.3)$$

The parameter C is equal to 1 or -1, according to whether the pump frequencies are in the normal- or anomalous-dispersion regime, respectively. The other

three variables have the form of wave-number shifts divided by the nonlinear wave-number shift imposed on each sideband by the appropriate pump wave. In terms of these dimensionless variables, Eq. (4.1) becomes

$$[K^2-C\Omega^2(2+C\Omega^2)][(K-2CS\Omega)^2-C\Omega^2(2+C\Omega^2)]$$

$$=(4\Omega^2)^2 . \quad (4.4)$$

Condition (4.2) requires that $S\gg 1$ and condition (3.10) requires that $\Omega<S/2$. First, suppose that $K\sim\Omega\sim 1$. Then the second group of terms in Eq. (4.4) is of order S^2 and the modulational interactions of the two pump waves decouple. For the lower-frequency pump wave, the reduced dispersion relation is

$$K=\pm[C\Omega^2(2+C\Omega^2)]^{1/2} . \quad (4.5)$$

When $C=1$, corresponding to normal dispersion, the

lower-frequency pump wave is stable. When $C = -1$, corresponding to anomalous dispersion, the lower-frequency pump wave is modulationally unstable by itself; the effects of cross-phase modulation are insignificant. Similar results apply to the higher-frequency pump wave. The approximation used in deriving Eq. (4.5) is self-consistent whenever

$$\left| \frac{4\Omega^2}{S^2 \pm S(2C + \Omega^2)^{1/2}} \right| \ll |\Omega^2(2C + \Omega^2)| . \quad (4.6)$$

Since condition (4.6) is satisfied for all $\Omega \leq S/2$, *no cross-phase-induced instability can exist*. Although this result was proved for a parabolic dispersion curve, the key ingredient is that the curvature of the dispersion curve not change sign in the aforementioned frequency range. Thus, we expect the stated result to be true for conventional fibers in general. When $S \sim 1$, the preceding analysis is not valid because pump-pump FWM occurs and Eqs. (3.3) and (3.4) do not describe an equilibrium solution of the Zakharov equation. However, the wave evolution for this case has been studied numerically by Rothenberg [5]. No evidence of modulational instability was found.

Figure 2(c) illustrates the case in which ω_1 is in the anomalous-dispersion regime and ω_2 is in the normal-dispersion regime. As shown in the figure, it is always possible to find pump frequencies for which the pump-wave group velocities are equal. This situation is similar to the one analyzed by Inoue [12]. In the spirit of the cases analyzed previously, suppose that the dispersion curve is parabolic in the vicinities of both pump frequencies. Then the dispersion equation (3.16) becomes

$$[K^2 - C_1\Omega^2(2 + C_1\Omega^2)][K^2 - C_2\Omega^2(2 + C_2\Omega^2)]$$
$$= (4C_1\Omega^2)(4C_2\Omega^2) , \quad (4.7)$$

where K and Ω are as defined in Eqs. (4.3) and

$$C_1 = \text{sgn}[\beta_2(\omega_1)] = -1 , \quad C_2 = \beta_2(\omega_2)/|\beta_2(\omega_1)| > 0 . \quad (4.8)$$

Since the pump frequencies are well separated, there is no reason to assume that the magnitudes of C_1 and C_2 are equal, as they were in the previous two cases. The solutions of Eq. (4.7) can be written in the form

$$2K^2 = [C_1\Omega^2(2 + C_1\Omega^2) + C_2\Omega^2(2 + C_2\Omega^2)]$$
$$\pm \{[C_1\Omega^2(2 + C_1\Omega^2) - C_2\Omega^2(2 + C_2\Omega^2)]^2$$
$$+ 4(4C_1\Omega^2)(4C_2\Omega^2)\}^{1/2} . \quad (4.9)$$

The most unstable branch of Eq. (4.9) is displayed in Fig. 3, for three values of C_2. The curve corresponding to $C_2 = 1$ is particularly interesting, because it seems to imply that instability exists for arbitrary values of the modulational frequency Ω. For future reference, notice that Eq. (4.9) reduces to $K \approx \pm(\Omega^2 \pm i\sqrt{3})$ when $C_2 = 1$ and $\Omega^2 \gg 1$. To understand this result, recall that the coupled modulational instability of two pump waves, which involves four sidebands, is comprised of three distinct two-sideband interactions. The modulational instability of the lower-frequency pump wave involves B_{1+}
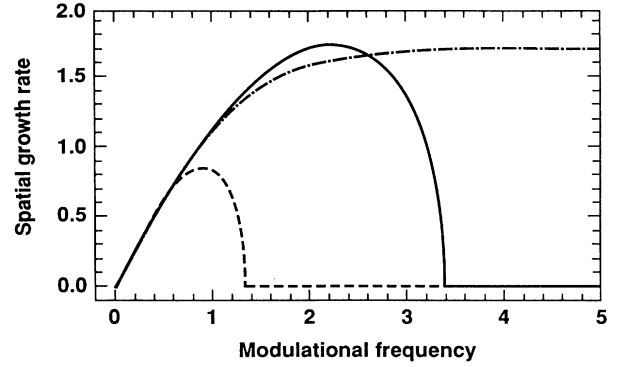

FIG. 3. Spatial growth rate plotted as a function of the modulational frequency for the case in which one pump frequency is in the normal-dispersion regime and the other pump frequency is in the anomalous-dispersion regime, and the pump-wave group velocities are equal. The normalizations of the spatial growth rate and the modulational frequency are given in Eqs. (4.3). The broken line corresponds to $C_2 = 2$, the dot-dashed line corresponds to $C_2 = 1$, and the solid line corresponds to $C_2 = 0.5$.

and B_{1-}, and is characterized by the wave-number mismatch

$$\Delta(1-,1+) = 2\beta(\omega_1) - \beta(\omega_1 + \omega) - \beta(\omega_1 - \omega)$$
$$\approx -\beta_2(\omega_1)\omega^2 . \quad (4.10)$$

A similar expression exists for the mismatch of the modulational instability of the higher-frequency pump wave. Forward FWM involves B_{1+} and B_{2-}, and is characterized by the mismatch

$$\Delta(2-,1+) = \beta(\omega_1) + \beta(\omega_2) - \beta(\omega_1 + \omega) - \beta(\omega_2 - \omega)$$
$$\approx [\beta_1(\omega_2) - \beta_1(\omega_1)]\omega$$
$$- [\beta_2(\omega_2) + \beta_2(\omega_1)]\omega^2/2 . \quad (4.11)$$

This interaction can be unstable. Bragg reflection involves B_{1+} and B_{2+}, is characterized by the mismatch

$$\Delta(2+,1+) = \beta(\omega_2) + \beta(\omega_1 + \omega) - \beta(\omega_1) - \beta(\omega_2 + \omega)$$
$$\approx -[\beta_1(\omega_2) - \beta_1(\omega_1)]\omega$$
$$- [\beta_2(\omega_2) - \beta_2(\omega_1)]\omega^2/2 , \quad (4.12)$$

and is intrinsically stable. For the case under discussion, only forward FWM is (linearly) phase matched when $\Omega^2 \gg 1$ and must be responsible for the predicted instability. The associated matching condition (4.11) is illustrated by Fig. 4. This argument can be quantified: If one retains only B_{1+} and B_{2-} in Eqs. (3.12), one obtains the dispersion equation

$$[K - (1 + C_1\Omega^2)][K + (1 + C_2\Omega^2)] = -4 , \quad (4.13)$$

which has the solution

$$K = (C_1 - C_2)\Omega^2/2 \pm i\{4 - [1 + (C_1 + C_2)\Omega^2/2]^2\}^{1/2} . \quad (4.14)$$
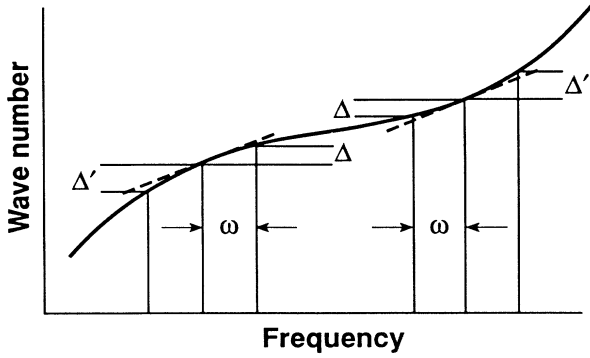
FIG. 4. Wave-number matching condition (4.11) illustrated for the case in which one pump frequency is in the normal-dispersion regime and the other pump frequency is in the anomalous-dispersion regime. The pump-wave group velocities are equal and $C_2 = 1$.

When $C_2 = 1$, $K = -\Omega^2 \pm i\sqrt{3}$, in agreement with the corresponding limit of Eq. (4.9). Having analyzed this two-sideband interaction quantitatively, one can now understand the stated result physically: When $C_2 = 1$, the dispersion curvatures associated with the frequencies $\omega_1 + \omega$ and $\omega_2 - \omega$ are equal and opposite, and the (linear) wave-number mismatch is identically zero for all values of ω. This degeneracy can be removed by retaining ω^3 terms in the matching condition (4.11). The other two curves in Fig. 3 correspond to coupled modulational instabilities. To see this, simply observe that neither curve has the precise shape required by Eq. (4.14), or by Eq. (4.5). [For the case in which $C_2 = 0.5$, the spatial growth rate predicted by Eq. (4.14) is a reasonable approximation to the exact growth rate in the range $\Omega > 3$.] Even though Eq. (4.14) does not predict these two curves accurately, one can still use it to gain some insight into the difference between them: When $C_2 = 2.0$, the linear and nonlinear mismatch terms in Eq. (4.14) reinforce one another, whereas when $C_2 = 0.5$, they oppose one another over a limited range of modulational frequencies. This observation is consistent with the fact that the range of modulational frequencies corresponding to instability is larger for the latter case than for the former. For cases in which $0 < |C_1| - C_2 \ll 1$, the linear mismatch term cancels the nonlinear mismatch term when the modulational frequency is large: Eq. (4.14) is relevant and the peak spatial growth rate of the instability is 2, rather than $\sqrt{3}$. Notice that the modulational frequency can have either sign; symmetric Stokes and anti-Stokes emission always occurs when the pump-wave group velocities are equal and the parabolic approximation is valid.

Now suppose that the pump-wave group velocities are unequal. Then the four-sideband interaction is governed by

$$[K^2 - C_1\Omega^2(2 + C_1\Omega^2)][(K - 2S\Omega)^2 - C_2\Omega^2(2 + C_2\Omega^2)]$$

$$= (4C_1\Omega^2)(4C_2\Omega^2) , \qquad (4.15)$$

where

$$S = \frac{\beta_1(\omega_2) - \beta_1(\omega_1)}{|2\gamma P \beta_2(\omega_1)|^{1/2}} \qquad (4.16)$$

characterizes the difference between the pump-wave group velocities. Forward FWM is described by Eq. (4.13), with $C_2\Omega^2$ replaced by $-2S\Omega + C_2\Omega^2$. Correspondingly, Eq. (4.14) becomes

$$K = S\Omega + (C_1 - C_2)\Omega^2/2$$

$$\pm i\{4 - [1 - S\Omega + (C_1 + C_2)\Omega^2/2]^2\}^{1/2} . \qquad (4.17)$$

It is evident from Eq. (4.15) that the modulational interactions of the two pump waves decouple when $|S| \gg 1$ and $\Omega^2 \sim 1$: the lower-frequency pump wave is modulationally unstable by itself, whereas the higher-frequency pump wave is modulationally stable. Since Eq. (4.15) is not biquadratic in k, it has no simple solutions to facilitate study of the regime in which $\Omega \gg 1$. However, it is clear from Eqs. (4.10)–(4.12) that the modulational instabilities of each pump wave are not (linearly) phase matched, and that forward FWM and Bragg reflection cannot be (linearly) phase matched simultaneously. Thus, only a forward FWM instability can exist, subject to the requirement that the dispersion coefficients have different magnitudes. Notice that the wave-number matching condition (4.11) requires the modulational frequency to have a definite sign; symmetric Stokes and anti-Stokes emission cannot occur. This conclusion also follows from Eq. (4.17). When Ω is positive, Eq. (4.17) corresponds to the interaction of B_{1+} and B_{2-}, as stated previously. When Ω is negative, Eq. (4.17) corresponds to the interaction of B_{1-} and B_{2+}. It has already been demonstrated that cross-phase-induced instability exists when $S = 0$. By continuity, we expect that cross-phase-induced instability can exist when $S \sim 1$, over a limited range of Ω. However, Eq. (4.15) must be solved numerically to obtain quantitative results.

In related work, Schadt and Jaskorzynska [13] considered the interaction of a strong pump pulse, propagating in the normal-dispersion regime, and a weak continuous signal wave, propagating in the anomalous-dispersion regime, with a group velocity comparable to that of the pump pulse. By numerically solving a pair of coupled NS equations, they showed that the cross-phase modulation imposed by the pump pulse on the signal wave induced the formation of a short signal pulse, even though the pump pulse had an intrinsic tendency to broaden and the signal wave was too weak to be modulationally unstable by itself. This effect has been demonstrated experimentally by Greer et al. [14]. The most unstable branch of Eq. (4.9) is displayed in Fig. 5(a) for $C_2/C_1 = -1.4$, the ratio used by Schadt and Jaskorzynska in their numerical simulations. Since the peak spatial growth rate of the instability and the range of modulational frequencies corresponding to instability are both larger than those of the modulational instability of the lower-frequency pump wave by itself [see Eq. (4.5)], the results of this paper are similar to those of Schadt and Jaskorzynska. However, a fairer comparison of the results requires a study of the cross-phase-induced instabilities for the case in which the lower-frequency pump wave
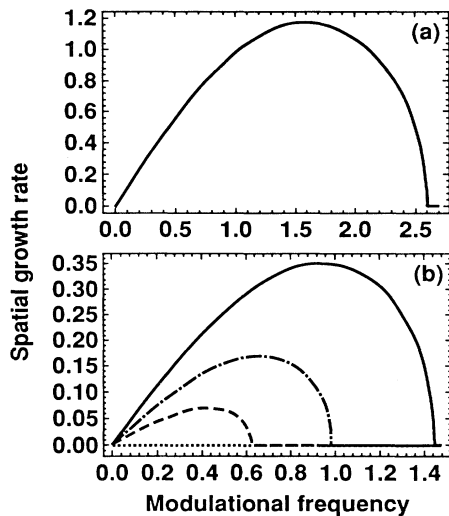
FIG. 5. Spatial growth rate plotted as a function of the modulational frequency for the case in which one pump frequency is in the normal-dispersion regime and the other pump frequency is in the anomalous-dispersion regime. The normalizations of the spatial growth rate and the modulational frequency are given in Eqs. (A2). The pump-wave group velocities are equal and $C_2/C_1 = -1.4$. (a) The power ratio of the lower-frequency to the higher-frequency pump wave $R = 1$. (b) The solid line corresponds to $R = 0.25$, the dot-dashed line corresponds to $R = 0.16$, the broken line corresponds to $R = 0.11$, and the dotted line corresponds to $r = 0.09$.

is much weaker than the higher-frequency pump wave. The details of such an analysis are given in the Appendix. The main results are twofold. When instability exists, the peak growth rate of the cross-phase-induced instability is larger than that of the modulational instability of the lower-frequency pump wave by itself, for most values of the pump-wave intensity ratio. However, no instability exists when the pump-wave intensity ratio is less than a certain critical value. These results are illustrated by Fig. 5(b). The latter result differentiates the physics of the instabilities of two continuous waves and the interaction of a continuous wave and a short pulse.

The frequency dependence of the natural wave number in a dispersion-flattened fiber [15] is shown in Fig. 6. There are two frequency domains in which the fiber exhibits normal dispersion, separated by a domain in which the fiber exhibits anomalous dispersion. The analysis of the cases in which one pump frequency is in the domain of anomalous dispersion and the other pump frequency is in either of the two domains of normal dispersion is identical to the corresponding analysis for light-wave propagation in a conventional fiber. Hence, it need not be discussed further. Figure 6 illustrates the case in which the pump frequencies are in separate domains of normal dispersion. It is clear from the figure that the pump frequencies can be chosen in such a way that the pump-wave group velocities are equal. The dispersion equation for this situation is Eq. (4.7), with $C_1 = 1$ and $C_2 > 0$. For the special case in which $C_2 = 1$, a cross-phase-induced modulational instability is known to occur [2,3]. Howev-
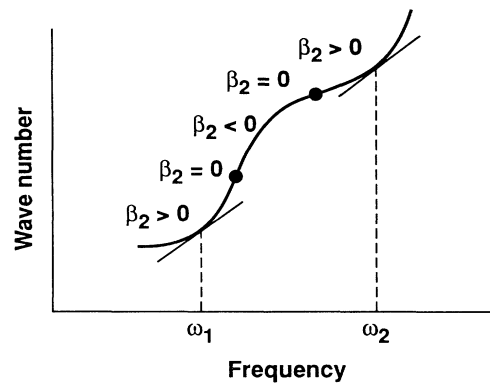

FIG. 6. Dispersion curve of a dispersion-flattened fiber. The two pump frequencies are in separate normal-dispersion regimes. Notice that the pump frequencies can be chosen in such a way that the pump-wave group velocities are equal.

er, since the pump frequencies are well separated, there is no reason to assume that the dispersion coefficients are equal. The spatial growth rate of the coupled modulational instability is displayed in Fig. 7, for three values of C_2. Varying C_2 alters the peak growth rate of the instability and the range of frequencies corresponding to instability. The latter effect can be understood qualitatively by regarding $(C_1 + C_2)/2$ as the effective dispersion coefficient; increasing the effective dispersion coefficient reduces the range of unstable wave numbers, whereas reducing the effective dispersion coefficient increases the range of unstable wave numbers, as is the case for a single modulationally unstable wave. However, the coupled modulational instability is less sensitive to the value of C_2 than are the instabilities associated with Fig. 2(c). In particular, there is no distinct forward FWM instability when $C_2 = 1$. This result also follows from Eq. (4.11).

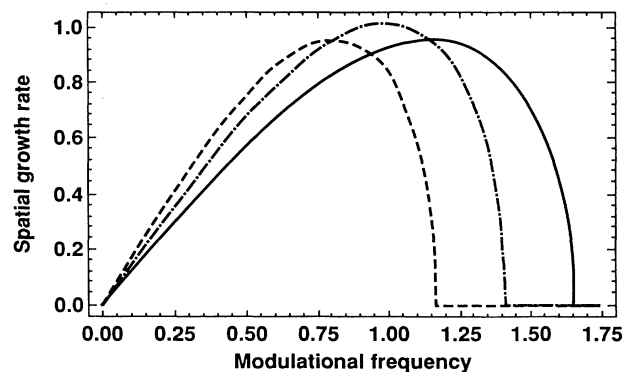Now suppose that the pump-wave group velocities are

FIG. 7. Spatial growth rate plotted as a function of the modulational frequency for the case in which the two pump frequencies are in separate normal-dispersion regimes and the pump-wave group velocities are equal. The normalizations of the spatial growth rate and the modulational frequency are given in Eqs. (4.3). The solid line corresponds to $C_2 = 0.5$, the dot-dashed line corresponds to $C_2 = 1.0$, and the broken line corresponds to $C_2 = 2.0$.

unequal. Then the four-sideband interaction is governed by Eq. (4.15), with S as defined in Eq. (4.16), $C_1 = 1$, and $C_2 > 0$. The interaction of B_{1+} and B_{2-} is governed by Eq. (4.17). Suppose, temporarily, that $C_2 = 1$. The dispersion equation for this case is mathematically equivalent to Eq. (4.4). It follows immediately that, when $|S| \gg 1$ and $\Omega \sim 1$, the modulational interactions of the two pump waves decouple and both pump waves are modulationally stable. When $\Omega \gg 1$, further analysis is required. Fortunately, the dispersion equation has the exact solution

$$(K - S\Omega)^2 = \Omega^2 (2C + \Omega^2) + (S\Omega)^2$$
$$\pm \{(4\Omega^2)^2 + 4(S\Omega)^2 [\Omega^2 (2C + \Omega^2)]\}^{1/2} ,$$
$$(4.18)$$

from which it follows that the condition

$$S^2 - 2C - 4 < \Omega^2 < S^2 - 2C + 4 \qquad (4.19)$$

must be satisfied for instability to exist. [Since condition (4.6) is only violated when $\Omega^2 + 2C \approx S^2$, one should not be surprised by condition (4.19).] From the discussion following Eq. (4.17), it follows that this instability is forward FWM. The agreement between the predictions of Eqs. (4.17) and (4.18) is evident in Fig. 8 and confirms the preceding assertion. In the present case, solutions (4.17) and (4.18) are meaningful because B_{1+} and B_{2-} are physically distinct from the two pump waves. One need only check that the modulational frequency is not so large that the Taylor expansion of the natural wave number, used in the derivation of Eqs. (4.4) and (4.15), is invalid. When S is positive, the mismatch terms in Eq. (4.17) cancel for $\Omega \approx S$. This cancellation results in a
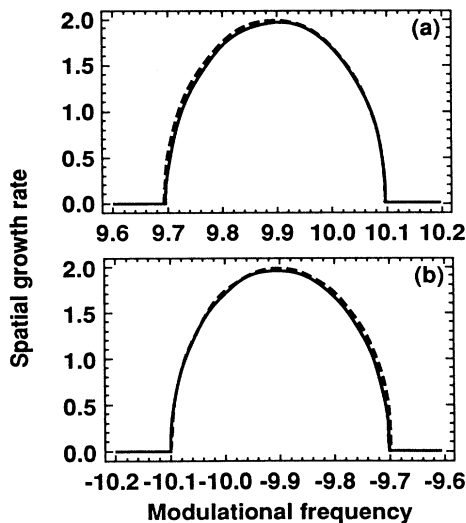

FIG. 8. Spatial growth rate plotted as a function of the modulational frequency for the case in which the two pump frequencies are in separate normal-dispersion regimes and the pump-wave group velocities are unequal. The normalizations of the spatial growth rate and the modulational frequency are given in Eqs. (4.3). The solid line corresponds to the exact result (4.18), whereas the broken line corresponds to the approximate result (4.17). (a) $S = 10$; (b) $S = -10$.

peak spatial growth rate of 2, as shown in Fig. 8(a). (In contrast, when $C_2 = -1$ such a cancellation does not occur and the peak spatial growth rate is $\sqrt{3}$.) When S is negative, the mismatch terms do not cancel for positive Ω, and the interaction of B_{1+} and B_{2-} is not phase matched. However, by changing the sign of the modulational frequency in Eq. (4.11), one can show that the interaction of B_{1-} and B_{2+} is phase matched. This change is equivalent to a change of sign of Ω in Eq. (4.17) and also results in a peak spatial growth rate of 2, as shown in Fig. 8(b). When $C_2 \neq 1$, solution (4.18) is no longer relevant. However, the decoupling of the two modulational interactions when $\Omega \sim 1$ is not sensitive to the value of C_2 and still occurs. The forward FWM instability is still governed by Eq. (4.17).

In other types of dispersive media, it is possible for the pump frequencies to be in separate anomalous-dispersion regimes. In this case, both pump waves are modulationally unstable by themselves. Cross-phase modulation couples the single-pump instabilities to produce a two-pump instability that has a larger spatial growth rate than either of the single-pump instabilities [2,3]. The analysis of this case is similar to that described in the preceding two paragraphs, as are the conclusions.

V. SUMMARY

The method of Zakharov was used to study instabilities induced by cross-phase modulation in a single-mode fiber. This method is valid for differences between the pump and sideband frequencies that are larger than those allowed in the usual NS analysis. Contrary to the predictions of coupled NS equations, the existence of cross-phase modulation does not guarantee the existence of instability.

If both pump frequencies are in the normal-dispersion regime of a conventional fiber, there is no instability. If both pump frequencies are in the anomalous-dispersion regime, the pump waves are modulationally unstable by themselves, but do not cooperate to produce a coupled modulational instability. For dispersive media in general, a sufficient condition for the existence of a (four-sideband) coupled modulational instability is that the difference between the pump-wave group velocities can be made small without producing pump-pump FWM. This situation can arise in a conventional fiber when the two pump frequencies are in different dispersion regimes (normal and anomalous).

The dispersion curve associated with a dispersion-flattened fiber has two regions in which dispersion is normal, separated by a region in which dispersion is anomalous. Coupled modulational instability can also occur in a dispersion-flattened fiber when the two pump frequencies are in different normal-dispersion regimes and the pump-wave group velocities are comparable.

In each type of fiber, the coupled modulational instability is suppressed by the presence of a large difference in the pump-wave group velocities. However, cross-phase modulation can still induce a (two-sideband) FWM instability.

The central theme of this paper is how dispersion con-

trols which of the three constituent two-sideband interactions are phase matched for a particular value of the modulational frequency. With dispersive effects replaced by geometric (diffractive) effects, this theme is also relevant to transverse instabilities of two copropagating light waves. These instabilities are analyzed in detail in Refs. [3], [4], and [16]–[18].

Note added in proof. The work of Huang and Hong [J. Lightwave Technol. **10**, 156 (1992)] has recently come to our attention. Their analysis is similar, but not identical, to the analysis of the present paper, and to that of Refs. [4] and [16].

ACKNOWLEDGMENTS

APPENDIX: UNEQUAL PUMP-WAVE POWERS

It follows from Eq. (3.16) and the assumption that the dispersion curve is parabolic in the neighborhoods of the pump frequencies that the dispersion equation for the four-sideband instability is

$$[K^2 - C_1\Omega^2(2R + C_1\Omega^2)][K^2 - C_2\Omega^2(2 + C_2\Omega^2)]$$
$$= R(4C_1\Omega^2)(4C_2\Omega^2) , \quad \text{(A1)}$$

where

$$K = \frac{k - \beta_1\omega}{\gamma P_2} , \quad \Omega = \left|\frac{\omega^2\beta_2(\omega_2)}{2\gamma P_2}\right|^{1/2} > 0 , \quad R = \frac{P_1}{P_2} ,$$
$$C_2 = \text{sgn}[\beta_2(\omega_2)] , \quad C_1 = \beta_2(\omega_1)/|\beta_2(\omega_2)| . \quad \text{(A2)}$$

All quantities in Eq. (A1) were normalized relative to those associated with the higher-frequency pump wave, because the comparison of this instability analysis with the work of Schadt and Jaskorzynska [13] is facilitated by holding P_2 fixed while P_1 is varied. The solution of Eq. (A1) is

$$2K^2 = [C_1\Omega^2(2R + C_1\Omega^2) + C_2\Omega^2(2 + C_2\Omega^2)]$$
$$\pm \{[C_1\Omega^2(2R + C_1\Omega^2) - C_2\Omega^2(2 + C_2\Omega^2)]^2$$
$$+ 4R(4C_1\Omega^2)(4C_2\Omega^2)\}^{1/2} . \quad \text{(A3)}$$

As mentioned in Sec. V, there are many similarities between modulational instabilities in which the linear wave-number mismatches (4.10)–(4.12) are due to dispersion and those in which the linear wave-number mismatches are due to diffraction. In particular, the dependence of the spatial growth rate of the coupled modulational instability on the pump-wave power ratio was studied in Refs. [3], [16], and [18] for the analogs of the cases in which both pump frequencies are in the normal or anomalous dispersion regime. The dependence of the spatial growth rate of the FWM instability on the pump-wave power ratio was studied in Refs. [4], [16], and [18]. Consequently, these cases need not be discussed herein.

For the case in which $C_2 = 1$ and $C_1 < 0$, it was determined empirically that instability occurs when the term in curly brackets in Eq. (A3) is negative. A necessary and sufficient condition for this to happen is that

$$7 + 4\sqrt{3} > |C_1 R| > 7 - 4\sqrt{3} . \quad \text{(A4)}$$

For Fig. 5, $C_1 = -0.714$. Correspondingly, the second of inequalities (A4) predicts that instability will occur when the pump-wave power ratio exceeds 0.100, in agreement with the figure. Further analysis of Eq. (A3) shows that the second of the inequalities (A4) is a sufficient condition for instability, for all negative values of C_1.

[1] G. P. Agrawal, *Nonlinear Fiber Optics* (Academic, Boston, 1989), Chaps. 2 and 7.
[2] G. P Agrawal, Phys. Rev. Lett. **59**, 880 (1987).
[3] C. J. McKinstrie and R. Bingham, Phys. Fluids B **1**, 230 (1989); **2**, 3215 (1990).
[4] C. J. McKinstrie and G. G. Luther, Phys. Scr. **T30**, 31 (1990). This paper contains a bibliography of early work on coupled modulational instabilities, to which should be added G. J. Roskes, Stud. Appl. Math. **55**, 231 (1976).
[5] J. E. Rothenberg, Phys. Rev. A **42**, 682 (1990).
[6] J. E. Rothenberg, Phys. Rev. Lett. **64**, 813 (1990).
[7] G. P. Agrawal, Phys. Rev. Lett. **64**, 814 (1990).
[8] V. E. Zakharov, Zh. Eksp. Teor. Fiz. **51**, 1107 (1966) [Sov. Phys. JETP **24**, 740 (1967)].
[9] V. E. Zakharov, Zh. Prikl. Mekh. Tekh. Fiz. **9**, 86 (1968) [J. Appl. Mech. Tech. Phys. **9**, 190 (1968)].
[10] H. C. Yuen and B. M. Lake, in *Advances in Applied Mechanics*, edited by C. S. Yih (Academic, New York, 1982), pp. 67–229. Pages 86–89 and 111–118 are of particular relevance.
[11] C. J. McKinstrie and M. V. Goldman, J. Opt. Soc. Am. B **9**, 1778 (1992).
[12] Y. Inoue, J. Phys. Soc. Jpn. **43**, 243 (1977).
[13] D. Schadt and B. Jaskorzynska, Electron. Lett. **23**, 1091 (1987).
[14] E. J. Greer, D. M. Patrick, P. G. J. Wigley, and J. R. Taylor, Opt. Lett. **15**, 851 (1990).
[15] G. P. Agrawal, *Fiber-Optic Communication Systems* (Wiley, New York, 1992), Chap. 2.
[16] G. G. Luther and C. J. McKinstrie, J. Opt. Soc. Am. B **7**, 1125 (1990).
[17] G. P. Agrawal, J. Opt. Soc. Am. B **7**, 1072 (1990).
[18] M. Kauranen, A. L. Gaeta, and C. J. McKinstrie, J. Opt. Soc. Am. B (to be published).